[•OH(X)] measurement by resonant absorption spectroscopy in a pulsed dielectric barrier discharge

C. Hibert, I. Gaurand, Olivier Motret, Jean Michel Pouvesle

[OH(X)] measurements by resonant absorption spectroscopy in a pulsed dielectric barrier discharge

C. Hibert,[a] I. Gaurand, O. Motret, and J. M. Pouvesle
GREMI, UMR 6606, Université d'Orléans, B.P. 6759, 45067 Orléans Cedex 2, France

(Received 4 September 1998; accepted for publication 2 February 1999)

Good understanding of the different phases of the plasma-chemistry involved is essential for the development of nonthermal plasma technologies for pollution control. These techniques are often based on the dissociation of parent gases to produce radicals that, in turn, decompose the toxic compounds. Our research concerns OH radical production in a pulsed dielectric barrier discharge (DBD). OH[$A\,^2\Sigma^+ - X\,^2\Pi(0,0)$] emission in argon-water vapor gas mixtures has been studied. Particular attention has been paid to the influence of water vapor partial pressure on the lifetime and intensity of emitted fluorescence in order to develop a pulsed DBD ultraviolet light source for spectroscopic investigation. This source was used to perform OH($X\,^2\Pi$) time-resolved average absolute density measurements in other DBD discharges based on resonant absorption spectroscopy. This diagnostic has been validated in argon and air-water vapor mixtures. The temporal behavior of the density OH($X\,^2\Pi$) radicals after a pulse discharge has been studied in argon and air with and without 500 ppm of trichloroethylene. This simple and inexpensive tool, compared to more sophisticated laser absorption or laser-induced fluorescence measurements for plasma investigation, is very useful for characterizing the OH radical potential for pollutant oxidation. © *1999 American Institute of Physics.* [S0021-8979(99)03110-2]

I. INTRODUCTION

Common techniques such as thermal oxidation are not an economically viable solution when treating very dilute waste in atmospheric gases, as in such a process all the molecules in the gas stream are heated. An alternative can be found in the use of nonthermal plasma. In this case, the energy is mainly used for producing energetic electrons, ions, excited species and free radicals that lead to the decomposition of the pollutant molecule.

Nonthermal plasmas are generally produced by e-beams, dielectric barrier discharges (DBDs), or corona discharges. Pollutants can be decomposed through different processes such as direct electron collision or reactions with reactive free radicals. The most efficient method is through a complete oxidation, leading to the formation of only H_2O, CO_2, and acid, which can be easily collected. This generates no undesirable by-products. However, when oxidation is not complete, the kinetic chain can lead to unwanted products such as phosgene in case of trichloroethylene (TCE) treatment.[1,2]

One of the most interesting oxidant agents is the OH radical. It is characterized by a high oxido-reduction potential. In this article, an OH(X) density measurement technique in a pulsed DBD is presented.

DBDs are usually generated at atmospheric gas pressure. At such a pressure, the breakdown results in a multitude of short-lived microdischarges of small diameter, around 100 μm. Both diameter and duration depend mainly upon the gas used, the pressure, the discharge gap, and the applied voltage. One can discern three main steps in the life cycle of each microdischarge: (1) ionization, excitation, and dissociation of gas species, (2) production of reactive species, and (3) reaction chemistry in volume.[3]

Many OH(X) concentration measurements have been done in the atmosphere[4–6] based on long-path absorption spectroscopy with laser emission at 308 nm. During the day, OH(X) radical density is nearly constant in the atmosphere with a value around $10^6\,cm^{-3}$, which contrasts with an atmospheric pressure discharge plasma, where densities are more in the range of 10^{12}–$10^{15}\,cm^{-3}$ with typical lifetimes not exceeding milliseconds.[7] A number of studies of OH(X) by laser-induced fluorescence (LIF) have been performed in flames. This technique affords high spatial and temporal resolution, but implies a rather complicated experimental arrangement.[8–10]

In this article, we present an average OH(X) density measurement technique based on resonant absorption spectroscopy. After reporting the effect of water vapor pressure on OH radical emission in argon-water vapor gas mixtures, we show how OH radical emissions in particular experimental conditions can be used as a ultraviolet (UV) pulse source for spectroscopic investigation. OH(X) time-resolved density measurements have been performed in humid argon (with and without 500 ppm of TCE) and in humid air (with and without 500 ppm of TCE). This new tool for plasma investigation will be very useful to characterize the OH radical potential for pollutant oxidation.

II. EXPERIMENTAL ARRANGEMENT

The experimental setup, shown in Fig. 1, comprises three main parts: two DBD driven reactors with their gas handling system and a spectroscopic arrangement. One

[a]Electronic mail: cyrille.hibert@univ-orleans.fr

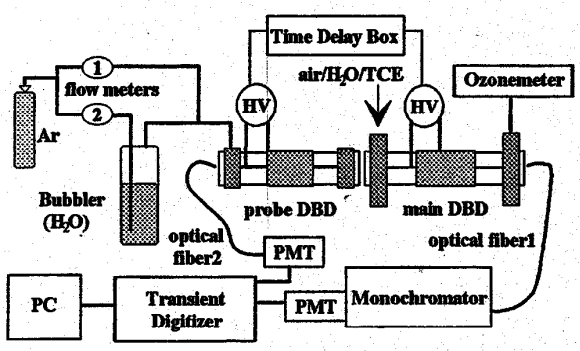

FIG. 1. Experimental setup.

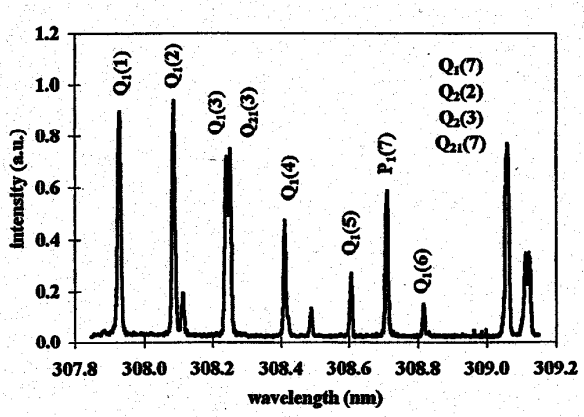

FIG. 2. Spectrum of the rotational bands of OH[$A\,^2\Sigma^+(v'=0)-X\,^2\Pi(v''=0)$].

DBD, named probe DBD, was used as the UV pulse source. The other one, named the main DBD, was used to study the production of hydroxyl radicals.

Both discharge cells were of coaxial geometry. Inner electrodes were made of tungsten wires (diameter 0.15 mm), outer electrodes were made from aluminium foils which were placed on dielectric Pyrex tubes with inner and outer diameters of 11 and 13 mm. Quartz windows were placed at all ends of cells to enable spectroscopic investigations. Both discharge gaps were set at 5.5 mm and the discharge volume was 10 cm^3 for the probe DBD and 19 cm^3 for the main DBD.

Cells were fed by two identical high voltage pulsers. Pulsed high voltage could reach 150 kV in open circuit with adjustable pulse frequency in the range 1 Hz–1 kHz (from 1 to 10 Hz in the present work). The voltage rise was of the order of 10^{12} V/s and pulse width of the voltage pulses was of the order of 50 ns. For a gap of 5.5 mm and at atmospheric pressure, breakdown voltage occurs at 10 kV, whereas a fast rising voltage allowed to reach a breakdown voltage between 10 and 50 kV, depending on the applied voltage. This kind of discharge is bipolar. The energy deposited per pulse in a cell can be adjusted in the range 0.016–1.6 J. Synchronization between the main DBD and the UV probe was achieved by the use of a tunable delay box triggered on the main discharge. During experiments, the delay between main discharge emission and probe emission was monitored on a fast transient digitizer. Jitter lower than 5 ns was measured between the two emissions.

Four gas flow controllers were used to make different gas mixtures in the two DBDs. Control of water vapor in the probe DBD was obtained with the mixture of two gas flows, one (F_1) of dry gas and the other one (F_2) of gas saturated with water vapor after bubbling. At room temperature (295 K), the vapor pressure of water is 27×10^{-3} bar.[11] The water vapor pressure in the gas was

$$P_{H_2O}=0.0027\times F_1/(F_1+F_2)(\text{bar}). \quad (1)$$

Two other gas flows were used to control water vapor pressure in the main DBD. In this experiment, we used high purity argon (less than 2 ppm water), argon containing 1000 ppm TCE, air containing 1000 ppm TCE supplied by Air Liquide Company and dry air.

The two discharges were placed in a Faraday cage to avoid electromagnetic perturbation.

Plasma emissions were observed with a SOPRA monochromator through the UV-visible optical fiber 1 (see Fig. 1). The monochromator covered the spectral range from 250 to 800 nm with a high resolution of about 40 000 in the second order. The signals from the photomultiplier tube (HAMAMATSU R955) were analyzed with a transient digitizer (Tektronix 520—bandwidth 500 MHz) connected to a personal computer. UV-visible plasma emission was monitored in the probe DBD discharge through optical fiber 2 connected to a fast photomultiplier tube from which the output signal served as a trigger signal for data acquisition. Such a device allowed the study of spectral emission for different time scales.

III. PROBE EMISSIONS

Formation of OH($A\,^2\Sigma^+$) has been extensively studied in e-beam excited argon-water vapor mixture for laser application in the UV range.[12,13]

We developed a UV pulse source (UV probe) based on the emission of OH($A\,^2\Sigma^+$), the first electronic excited state of OH radical emission, generated in atmospheric argon-water vapor mixture discharge.

We first studied the fluorescence of the ($A\,^2\Sigma^+,v=0$)–($X\,^2\Pi,v=0$) transition of OH radical in Ar–H_2O mixture. Figure 2 shows a high-resolution time-integrated emission spectrum obtained with 500 ppm of water vapor in an atmospheric argon plasma (gas flow of 500 cc/min, repetition rate of 10 Hz, and applied voltage of 30 kV). This spectrum has been used for rotational temperature calculation.[14]

The temporal evolution of the OH[$A\,^2\Sigma^+-X\,^2\Pi,0-0,Q_1(2)+Q_{21}(2)$] has been studied as a function of the water concentration in Ar. Q branch corresponds to transition $K\rightarrow K$, where K is the angular momentum.[15] These two lines cannot be separated because their emissions occurred at very close wavelength. The $Q_1(2)$ line has been selected for our applications because of its high intensity in our experimental conditions and because of the large absorption cross section of the corresponding

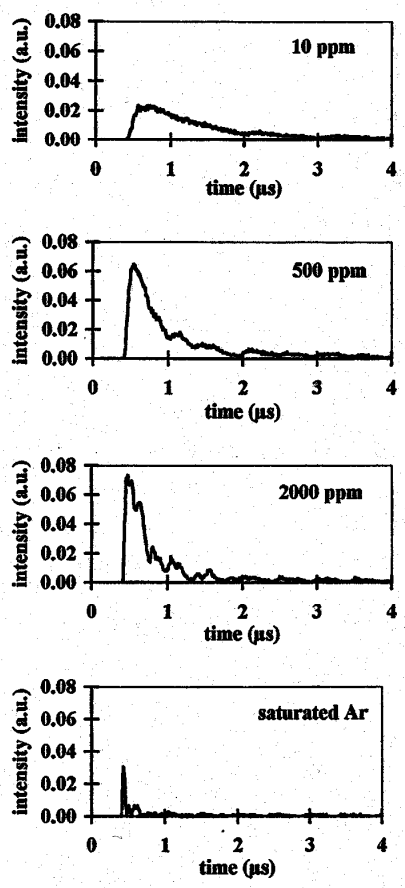

FIG. 3. Temporal evolution of the $Q_1(2)$ line as function of the water concentration.

transition. Figure 3 presents the temporal evolution of the $Q_1(2)$ branch at 308 nm for different values of water vapor pressure (64 mJ/pulse into the gas). The signal duration decreases with increasing water concentration. It varies from around 1 μs at very low water vapor pressure, to a few tens of nanoseconds at saturation. The intensity of the fluorescence rises with the increase in the water vapor pressure up to an optimum at around 200 ppm.

In fact, $OH(A\,^2\Sigma^+)$ emissions are mainly dependent on the following reactions:

$$Ar^*(4p)+H_2O \rightarrow Ar(3p)+OH^*(A\,^2\Sigma^+)+H, \quad (2)$$

$$OH^*(A\,^2\Sigma^+)+H_2O \rightarrow OH(X\,^2\Pi)+H_2O. \quad (3)$$

There is an equilibrium between $OH(A\,^2\Sigma^+)$ production in reaction (2) and the quenching of $OH^*(A\,^2\Sigma^+)$ with water molecules in reaction (3). A simple model based on these considerations has been proposed, it is in good agreement with experimental results.[16]

This study demonstrates that a very reproducible relation can be obtained between the duration of pulsed OH radical emissions and water vapor pressure. For example, at 500 ppm water vapor, the full width at half maximum (FWHM) of the pulse is 300 ns. The DBD probe can be considered as a UV pulse source resonant with $OH(A\,^2\Sigma^+)$ emissions. The next paragraph presents a technique for $OH(X\,^2\Pi)$ measurement using the DBD probe.

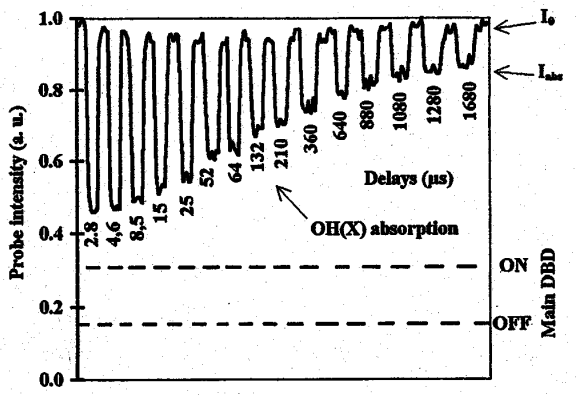

FIG. 4. Experimental resonant absorption result in saturated argon-water vapor mixture at atmospheric pressure.

IV. [OH(X)] MEASUREMENTS

A. OH(X) detection

The OH(X) density measurements are based on time-resolved resonant absorption spectroscopy using the experimental device in Fig. 1. OH rotational lines $Q_1(2)$ and $Q_{21}(2)$ of the $[A\,^2\Sigma^+ - X\,^2\Pi(0,0)]$ transition generated in the probe DBD were selected for the detection of OH(X) in the main DBD. Working water vapor pressure was 2×10^{-4} bar (200 ppm) in the probe DBD corresponding to the maximum OH radical emission.

The experimental method to detect OH(X) absorption is straightforward. The signal from the probe DBD was analyzed with and without the main discharge on, for different delays. That allowed the detection of OH(X) radical during the post discharge. Data acquisitions were triggered on probe emissions from optical fiber 2 and optical fiber 1 collected probe photons after going through the main DBD.

Figure 4 shows an experimental result obtained from a water vapor saturated argon mixture with a flow of 600 cc/min in the main discharge. Applied voltage was around 20 kV. This graph shows the temporal absorption of OH(X) radical. On this figure, we can see a good stability of the probe DBD emission level without absorption that lasts during the entire series of measurements. The temporal absorption of OH(X) decreased with time. Absorption reached 50% for delays around 1 μs. At 1680 μs, there is still a significant absorption of around 10%.

We checked that the absorption measured was due only to OH(X) radicals through different experiments. No absorption in dry argon was detected. Absorption was studied on different rotational lines Q_1 and led to identical results. In a final step, we checked that we were not in a saturation absorption regime.

All these observations show that the diagnostic developed allows the detection of OH(X) in an atmospheric pressure plasma discharge.

B. Signal analysis

OH(X) density measurements have been carried out using the Lambert–Beer law. Knowledge of the line shape is needed for absorption calculation.

1. Line shape function

The experimental rotational line $Q_1(2)+Q_{21}(2)$ shape function is the convolution between the monochromator shape function and the local emission line shape function $V_{Ei}(\lambda)$.

In our experimental conditions (atmospheric pressure, $T_{gas}\approx T_{room}$, low electron density$\leqslant 10^{14}\,cm^{-3}$), rotational lines were mainly broadened by pressure and Doppler effects. The local emission shape line function has been fitted with a Voigt profile resulting from the convolution of a Lorentzian profile (pressure) with a Gaussian profile (Doppler). At room temperature, Doppler broadening was low, around 0.001 nm (at 300 K). At atmospheric pressure, pressure broadening was around 0.002 nm.[17]

Experimental line shape function has been reconstructed using the convolution of a Lorentzian function (pressure) and a Gaussian function (Doppler + apparatus monochromator) as follows:

$$V(\Lambda)=\int_{-\infty}^{+\infty} G(\lambda)L(\Lambda-\lambda)d\lambda, \tag{4}$$

where V is a Voigt profile, G a Gaussian profile, and L a Lorentzian profile. Calculated Voigt profiles were compared to experimental ones. The best fit was obtained for a FWHM of the local shape equal to 0.0033 nm.

2. Lambert–Beer law

The probe DBD intensity $I_0(\lambda)$ at wavelength λ before the main DBD plasma is

$$I_0(\lambda)=\sum_{i=1}^{2} I_{0i}\,V_{Ei}(\lambda), \tag{5}$$

where I_{0i}=total energy of each line, where $i=1$ and 2 refers to $Q_1(2)$ and $Q_{21}(2)$ lines, respectively. $V_{Ei}(\lambda)$=local line emission shape function of the line considered.

The probe DBD intensity after absorption in main DBD can be expressed as,

$$I(\lambda)=\sum_{i=1}^{2} I_{0i}(\lambda)\exp\left[-\left(\frac{\Delta n}{n}\right)n\sigma_i(\lambda)l\right], \tag{6}$$

where $(\Delta n/n)$=the fraction of population residing in the rotation level from which the absorption transition originates, $(\Delta n/n)=0.1$ at 300 K,[4] n=the concentration of the absorbing species (cm^{-3}), l=the absorption path length in the main discharge (cm), $\sigma_i(\lambda)$=the cross section for the absorption transition, $\sigma_i(\lambda)=\sigma_{0i}V_{Ai}(\lambda)$, where σ_{0i}=the total cross section for the absorption transition i, $\sigma_{01}=6.146\times10^{-25}\,cm^2$,[18] $\sigma_{02}=2.105\times10^{-25}\,cm^2$,[18] $V_{ai}(\lambda)$=the absorption line shape function. We assumed the absorption function has the same shape as the emission function.

The relation between the OH(X) density and absorption A is

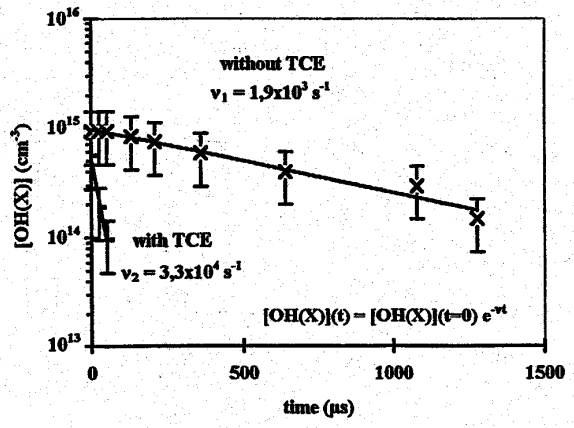

FIG. 5. Temporal evolution of average OH(X) density in saturated argon-water vapor mixture (27 000 ppm) with and without 500 ppm TCE at atmospheric pressure.

$$A=1-\sum_{i=1}^{2}\int_{-\infty}^{+\infty} I_{0i}(\lambda)\exp\left[-\left(\frac{\Delta n}{n}\right)n\sigma_i(\lambda)l\right]d\lambda. \tag{7}$$

Monochromator's slits have been adjusted in order to integrate the two lines $Q_1(2)$ and $Q_{21}(2)$.

3. Uncertainties

The dominant sources of error in OH(X) density measurements resulted from the experimental uncertainties on one hand, due to the relative stability of probe emissions. Experimental errors on the absorption could be estimated at 10%. On the other hand, we took into account errors from the line shape function calculations. A systematic error on OH(X) densities (in the range of 10^{13}–$10^{15}\,cm^{-3}$) of 50% was assumed, which is considering these two factors as main sources of errors.

For an absorption length of 20 cm, an absorption of 5% corresponds to an average OH(X) density of $5\times10^{13}\,cm^{-3}$, which represents the smallest concentration detectable in our experimental conditions. The highest absorption value that can be reasonably taken into account is around 85%, which corresponds to a concentration equal to $2\times10^{16}\,cm^{-3}$.

V. VALIDATION OF THE METHOD IN AR–H_2O MIXTURE

Different experiments were done in argon-water vapor mixture to validate the diagnostic that has been developed. Discharges in such a gas mixture generate no undesirable products that could absorb at the same wavelength as OH radical.

Figure 5 shows OH(X) density temporal evolution after a pulse discharge. The experimental conditions were as follows: 1200 cc/min argon flow containing 13 500 ppm water vapor, applied voltage of 20 kV, energy deposition per pulse of 36 mJ, and pulse voltage frequency of 10 Hz. This experiment was done with and without 500 ppm of TCE. The OH(X) density 1 μs after the pulse discharge was measured to be about $10^{15}\,cm^{-3}$. [OH(X)] temporal evolution

could be fitted with an exponential function. The measured destruction frequency of OH(X) was of the order of $1.9\times10^{3}\,s^{-1}$ without TCE and of the order of $3.3\times10^{4}\,s^{-1}$ with 500 ppm TCE. Then, if we consider that the TCE concentration is nearly constant in these experimental conditions, this corresponds to a rate coefficient $k_{\text{exp OH(X)TCE}}=2.7\times10^{-12}(\pm1.7\times10^{-12})\,cm^3/s$, which is in good agreement with values found in the literature $k_{(\text{OH TCE,300 K})}=2.2\times10^{-12}\,cm^3/s$.[19]

The influence of voltage and water vapor pressure on OH(X) production has been studied in argon at atmospheric pressure. The initial OH(X) density (1 μs after the pulse discharge, applied voltage 20 kV, and gas flow 1000 cc/min) was found to be around $10^{14}\,cm^{-3}$ for water density around $2.5\times10^{15}\,cm^{-3}$ (100 ppm) and increased to a value of $10^{15}\,cm^{-3}$ at saturated water vapor (27 000 ppm). For applied voltages between 10 and 50 kV (at saturated water vapor), OH(X) density (25 μs after the main discharge and for a gas flow of 1000 cc/min) was in a range of $4\times10^{14}-10^{15}\,cm^{-3}$. We observed a saturation around $10^{15}\,cm^{-3}$ for applied voltages above 30 kV.

Hydrogen peroxide dissociation leads to the formation of two OH radicals. An experiment was therefore performed with argon, water vapor, and hydrogen peroxide trace mixture. A liquid mixture H_2O/H_2O_2 (50% H_2O_2 per volume) was used in a bubbler. OH(X) density (3 μs after the main discharge, gas flow of 600 cc/min, and applied voltage of 20 kV) with and without hydrogen peroxide was around $10^{15}\,cm^{-3}$. H_2O_2 density in the gas mixture could not be easily estimated, but was low compared to water vapor density because of its low saturation pressure.[11] Nevertheless, a low H_2O_2 density influenced the OH(X) lifetime through the following reaction:[20]

$$\text{OH}(X)+H_2O_2\rightarrow HO_2+H_2O,\qquad k(300\ \text{K})=1.7\times10^{-12}\ cm^3/s. \tag{8}$$

Lifetime was around 200 μs with H_2O_2 trace and around 1 ms without.

These experiments validate the diagnostic developed and show that it is well adapted for OH(X) density measurements in discharges.

VI. APPLICATION IN AIR-WATER VAPOR MIXTURE

In real cases, pollutants are mostly diluted in air mixture. This section presents OH(X) density measurements in the main DBD containing air-water vapor mixture with and without TCE.

In air discharges OH radicals are mainly generated by the following reactions:[20]

$$e+H_2O\rightarrow OH+H+e,\quad k(300\ \text{K})=2\times10^{-9}\ cm^{-3}/s; \tag{9}$$

$$\text{O}(^1D)+H_2O\rightarrow OH+OH,\qquad k(300\ K)=1.6\times10^{-12}\ cm^3/s. \tag{10}$$

O(^1D) atoms are quenched by nitrogen or oxygen molecules to form the ground state O(^3P). O(^3P) atoms lead to the formation of ozone through the following reaction:[20]

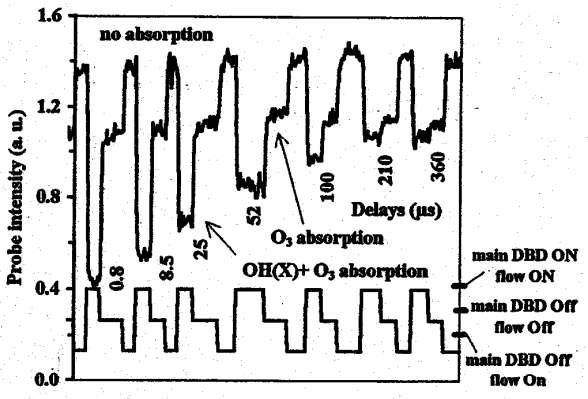

FIG. 6. Experimental resonant absorption result in saturated air-water vapor mixture at atmospheric pressure.

$$\text{O}(^3P)+O_2+M\rightarrow O_3+M,\qquad k(300\ \text{K})=6.9\times10^{-34}\ cm^6/s. \tag{11}$$

Ozone has a total absorption cross section around $10^{-20}\,cm^2$ at 308 nm.[21] Ozone absorption must be taken into account for OH(X) measurement in air-water vapor mixture. The contribution of both OH and ozone absorption at 308 nm must be evaluated. This was possible because of the very long lifetime of ozone compared to that of OH. To detect only ozone absorption, we simply had to simultaneously stop the gas flow and turn off the main discharge. This is illustrated on Fig. 6 (applied voltage of 30 kV, gas flow of 1000 cc/min, and air at atmospheric pressure containing 27 000 ppm water vapor). It can be seen that ozone absorption does not depend on delay. The ozone density is rapidly established and remains constant in the cell only a few seconds after the start of the main DBD. OH(X) could be well detected in only the first 200 μs.

An experiment has been performed in a mixture containing 500 ppm TCE to check if only OH(X) was detected. Figure 7 presents the temporal evolution of OH(X) density

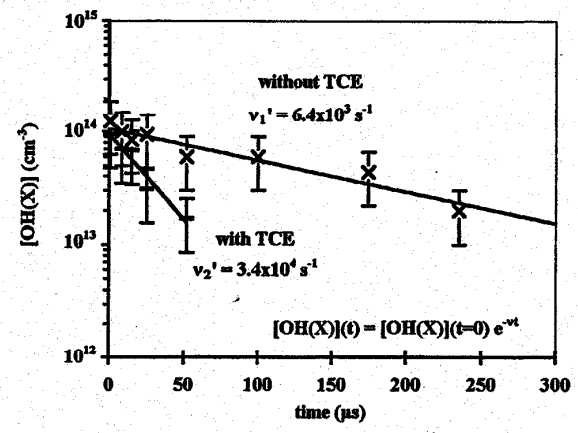

FIG. 7. Temporal evolution of average OH(X) density in saturated air-water vapor mixture (27 000 ppm) with and without 500 ppm TCE at atmospheric pressure.

TABLE I. Ozone and OH(X) concentration as function of the applied voltage (experimental conditions: water saturated air, gas flow of 600 cc/min and frequency of 10 Hz.

Applied voltage (kV)	$[O_3]$ (g/m^3)	$[OH(X)](t=25\ \mu s)$ (cm^{-3})	Destruction frequency (s^{-1})
22	1.8	8.5×10^{13}	3 600
29	3.8	2.4×10^{14}	10 800
36	5.7	5.6×10^{14}	18 500
43	6.5	1.3×10^{15}	25 000

with and without 500 ppm TCE (air containing 13 500 ppm water vapor at a flow of 1200 cc/min, applied voltage of 30 kV and pulse voltage frequency of 10 Hz).

Experimental results lead to a reaction rate of $k'_{\text{exp OH-TCE}}=2.2\times10^{-12}(\pm1.7\times10^{-12})\,\text{cm}^3/\text{s}$, which is in good agreement with the value previously measured in argon/H_2O/TCE mixture and with the literature value.[19] This experiment enabled us to validate the OH(X) density measurements in air discharge.

Figure 7 shows the initial OH(X) density around $10^{14}\,\text{cm}^{-3}$. This value is much smaller than the one obtained in argon for the same conditions. This is mainly due to the difference in the kinetic mechanisms occurring in the two mixtures. Indeed, in air discharges a considerable loss of energy occurs through: (1) rotational and vibrational excitation of nitrogen and oxygen molecules, and (2) oxygen dissociation, leading to the formation not only of OH but also of ozone. In air-water vapor mixture, the OH(X) lifetime was found to be around 100 μs, which is very short compared to the case of argon mixture. This is mainly due to the following reactions:

$$\text{OH}(X)+\text{O}_3\rightarrow\text{HO}_2+\text{O}_2,\qquad k(300\ \text{K})=6.8\times10^{-14}\ \text{cm}^3/\text{s};\tag{12}$$

$$\text{OH}(X)+\text{O}\rightarrow\text{H}+\text{O}_2,\qquad k(300\ \text{K})=3.3\times10^{-11}\ \text{cm}^3/\text{s}.\tag{13}$$

The effect of applied voltage on ozone and OH(X) production has been studied in air containing 27 000 ppm water vapor. Table I sums up the main results. The OH(X) destruction frequency depended strongly on ozone density through reaction (12).

VII. CONCLUSION

Time-resolved measurements of OH(X) radical average densities have been performed in high pressure high voltage triggered dielectric barrier discharge using resonant absorption spectroscopy. The OH($A-X$) fluorescence was furnished by a second identical DBD exciting an optimized mixture of argon and water vapor. The diagnostic developed has been applied to the study of the OH(X) reaction kinetics in different mixture containing various concentrations of water molecules. After validation of the method in Ar–H_2O and air–H_2O mixtures, the reaction rate of OH(X) with TCE has been measured in different experimental conditions. The very good agreement with the values previously published in the literature confirms that this simple method is well adapted to the diagnostic of high pressure nonequilibrium plasmas and can be extended to the characterization of other types of reactors. The results obtained an OH(X) lifetime at atmospheric pressure clearly show that at low concentrations of pollutants, the diffusion of OH radicals must be taken into account, leading to a chemistry not confined to the microdischarges volume.

ACKNOWLEDGMENTS

This work is supported by the Air Liquide Company and the Région Centre. The authors thank Elisabeth Jolivet for helping to improve the english of the article.

[1] D. Evans, L. Rosocha, G. Anderson, J. Coogan, and M. Kushner, J. Appl. Phys. **74**, 5378 (1993).
[2] A. C. Gentile and M. Kushner, J. Appl. Phys. **78**, 2977 (1995).
[3] B. Eliasson, M. Hirth, and U. Kogelschatz, J. Phys. D **20**, 1421 (1987).
[4] G. Hübler, D. Perner, U. Platt, A. Tönnissen, and D. H. Ehhalt, J. Geophys. Res. **89**, 1309 (1984).
[5] U. Platt, M. Rateike, W. Junkerman, J. Rudolph, and D. H. Ehhalt, J. Geophys. Res. **93**, 5159 (1988).
[6] D. M. Bakalayar, J. V. James, and C. C. Wang, Appl. Opt. **21**, 2901 (1982).
[7] A. Ershov and J. Brysow, J. Phys. D: Appl. Phys. **28**, 68 (1995).
[8] C. C. Wang and L. I. Davis, Jr., Appl. Phys. Lett. **25**, 34 (1974).
[9] M. Idir, Ph.D. thesis, de l'Université d'Orléans, 1995.
[10] J. J. Coogan and A. D. Sappey, IEEE Trans. Plasma Sci. **24**, 1 (1996).
[11] *American Institute of Physics Handbook*, edited by D. E. Gray (McGraw–Hill, New York, 1967).
[12] J. B. Leblond, F. Collier, F. Hofbeck, and P. Cottin, J. Chem. Phys. **74**, 6242 (1981).
[13] K. Tabayashi and K. Shobatake, J. Chem. Phys. **88**, 835 (1988).
[14] O. Motret, C. Hibert, S. Pellerin, M. Nikravech, and J. M. Pouvesle, C. R. Acad. Sci., Ser. IIb: Mec., Phys., Chim., Astron. **323**, 529 (1996).
[15] G. H. Dieke and H. M. Crosswhite, J. Quant. Spectrosc. Radiat. Transf. **2**, 97 (1962).
[16] C. Hibert, O. Motret, M. Nikravech, and J. M. Pouvesle, Cinquième Congrès de la Section Plasma (SFP), Autrans, 1997 (unpublished).
[17] E. Wennberg *et al.*, Rev. Sci. Instrum. **65**, 1858 (1994).
[18] H.-P. Dorn, R. Neuroth, and A. Hofzumahaus, J. Geophys. Res. **100**, 7397 (1995).
[19] B. M. Penetrante, M. C. Hsiao, J. N. Bardsley, B. T. Merritt, G. E. Vogtlin, A. Kuthi, C. P. Burkhart, and J. R. Bayless, Plasma Sources Sci. Technol. **6**, 251 (1997).
[20] R. Peyrous, P. Pignolet, and B. Held, J. Phys. D: Appl. Phys. **22**, 1658 (1989).
[21] N. J. Mason and S. Pathak, Contemp. Phys. **38**, 289 (1997).